Wearable Upper Arm SpO_2 Sensor for Wellness Monitoring

Matti T. Kinnunen[1], Mohammad H. Behfar, Nuutti Santaniemi, Tuomas Happonen, Dung Nguyen, Joni Kilpijärvi, Tommi Jaako, Jukka Happonen, Monica K. Russell, Christian A. Clermont, Michael J. Asmussen, Trevor A. Day, Markus Tuomikoski, Jussi Hiltunen

Abstract*—*Objective: **This paper describes the full development of a sensor for measuring optical heart rate (OHR) and blood oxygen saturation (SpO_2).** ***Methods:*** **A wearable sensor with a new type of skin compatible dispensed lens was designed and manufactured. All critical optical components, light emitting diodes (LEDs) and photodiode (PD) were close to skin and gave maximum light intensity due to minimal loss in the lens structure. Lens and optical components formed a thin monolithic structure.** ***Results:*** **Suppressed crosstalk between LED and PD was achieved by using two types of dispensed material: light blocking and transparent. High signal to noise ratio (SNR) and amplitude in the alternating current (AC) part of the photoplethysmography (PPG) signal were achieved. User comfort was achieved by having a small sensor located on the upper arm. When re-training the algorithm from our first iteration, the multiwavelength PPG sensor showed an SpO_2 RMSE of 2.61% with a 7-second average analysis for 25 participants. The average RMSE of heart rate over all 25 participants was 1.6 ± 1.1%.** ***Conclusion:*** **This study demonstrates a sensor with a clinical grade SpO_2 measurement and a highly accurate OHR measurement that is also comfortable and easy to wear.** ***Significance:*** **A dispensing method provides a new way of manufacturing sensor elements for wearable sensors with increased performance with reduced crosstalk.**

***Index Terms*—Heart rate, optical sensors, pulse oximetry, wearable sensors**

I. Introduction

People are increasingly interested in monitoring health and wellness and tracking their movements, activity, and training [1]. Typical wearable devices can monitor blood volume changes optically using a technique referred to as photoplethysmography (PPG). This technique can be implemented at rest and during sport activities. Recent wearable devices might show inaccuracy in PPG measurements due to several factors such as diverse skin pigmentation, motion artifacts, and signal crossover [2],[3]. It is known that physical activity decreases sensory accuracy [4]. Despite this limitation, researchers have been able to accurately measure HR optically with PPG during moderate to high physical activity at the upper arm, forearm, and temple locations [4],[5].

The latest improvements in the development of wearable devices have been the reduction of battery consumption, an increase in the number of different measurable physiological variables (e.g., measure electrocardiogram (ECG), bioimpedance, blood oxygen saturation (SpO_2)), and improvements in accuracy and user comfort. A wearable device can provide SpO_2 measurements for multiple applications such as endurance sport monitoring, high-altitude training [6], monitoring recovery after diving [7] as well as general health and medical applications like detecting indicators of sleep apnea [8]. Previously, measures of SpO_2 have been mostly used in clinical settings, such as in operating rooms [9],[10], during patient transport [11], and for home-oxygen therapy with the goal to improve patient safety [12]. Although the requirements for accuracy are less strict for consumer applications, measurement accuracy is still critical, and sensor validation will give clear benefits for the user. This area of development is evolving and only a few studies on validation of wearable SpO_2 devices can be found, where the readings are comparable to the reference medical pulse oximetry [13],[14],[15],[16].

Previous research has indicated that the sensor location influences measurement accuracy. Due to the usage of PPG for tracking HR in commercial wrist-worn devices (e.g., Apple, Garmin, Samsung, Polar), it is practical to measure SpO_2 from the wrist [17]. Instead of using a common wrist worn PPG sensor, an upper arm sensor provides a good alternative for reducing motion artifacts [18],[19],[20]. Even though, hypothetically speaking, the upper arm is a good alternative for

Manuscript received 26 July 2024; revised 11 November 2024; accepted 10 December 2024. Date of publication …. This work was supported by the European Union's Horizon 2020 research and innovation programme under Grant Agreement with No 871345 (www.medphab.eu). The authors would like to acknowledge Jennifer M. Demarty, Leo C. Transfiguracion, Breann R. Worobets, and Mark E. Pineda for their integral help and expertise with data collection from the multiwavelength PPG sensor SpO_2 validation project.

Matti Kinnunen, Nuutti Santaniemi, Joni Kilpijärvi, Tommi Jaako and Jukka Happonen are with the Polar Electro Oy, Kempele, Finland. (correspondence email: mattitapanikinnunen@hotmail.com).

Mohammad Behfar, Tuomas Happonen, Dung Nguyen, Markus Tuomikoski, and Jussi Hiltunen are with the VTT Technical Research Centre of Finland Ltd, Oulu, Finland.

Monica K. Russell, and Christian A. Clermont are with the Canadian Sport Institute Alberta - Sport Product Testing, Calgary, Alberta, Canada. Christian A Clermont is also with the Faculty of Kinesiology, University of Calgary, Calgary, Alberta, Canada.

Michael J. Asmussen is with the Faculty of Kinesiology, University of Calgary, Calgary, Alberta, Canada and with the Department of Kinesiology, Faculty of Education, Vancouver Island University, Nanaimo, British Columbia, Canada.

Trevor A. Day is with the Department of Biology, Faculty of Science and Technology, Mount Royal University, Calgary, Alberta, Canada and with the Department of Physiology and Pharmacology, Cumming School of Medicine, University of Calgary, Calgary, Alberta, Canada

sensor location, there is a paucity of research investigating the feasibility of SpO_2 measurement from the arm [13].

In this study, we characterize an optical sensor designed for sport, wellness, and health applications while maintaining clinical grade SpO_2 accuracy. The novel aspects of this sensor include a new optical configuration, and the usage of dispensing tools to manufacture sensor covers and optical lenses. This monolithic type of configuration enables robust positioning of LEDs, light barriers and lenses with a reduced number of discrete components simplifying the device assembly. A thinned structure can also improve the light delivery into the tissue of interest without an observable crosstalk between the light sources and the detectors. Additionally, the small size of the sensor makes it comfortable to wear and practical to use. The sensor can be placed freely, but we selected the upper arm to acquire more knowledge about this location for optical sensors and SpO_2 measurement. According to literature and the authors' experience, there is a possibility of getting better measurement performance at the upper arm compared to the wrist. [21] Benefits of the sensor are discussed in the context of sport-related applications.

II. Methods

Wearable optical heart rate measurement is typically using green LEDs for HR measurement and LEDs at red and infrared wavelengths for measuring oxygen saturation. LED light is used to detect volumetric changes of blood in microvascular tissue [22]. Theory, technology and applications of pulse oximetry as well as optical heart rate measurement have been extensively reviewed in the literature [9],[10],[23][24][25][26].

A. Sensor design, manufacturing, and verification

The multiwavelength PPG sensor was designed based on the commercially available components. A picture of the device can be seen in Fig. 1. Printed circuit boards (PCBs) were designed and manufactured using standard commercial manufacturing methods. Good optomechanical design of the sensor is essential for achieving high AC and good SNR [27]. The distance between the PD and LED is important and to get high-quality results, two pairs of RED/IR LEDs with two distances were used. One important aspect when designing the lens part is crosstalk minimization, as light can travel to the PD directly without going in the skin. Crosstalk reduces the dynamic range of the amplifier. Moreover, this unwanted signal can be modulated by movement of the skin under the sensor and cause additional artifacts. Thus, light barriers need to be optimized. Extra care in designing and manufacturing was employed to block light going directly from LED to PD. One more design target was to obtain optical components as close to the skin as possible to allow maximum light intensity coupled to skin. Optical distance needs to be as short as possible. Low profile surface mountable LEDs have wide radiation angle, so a low-profile lens maximizes the amount of light coupled to the skin and not in the lens materials. Three green LEDs were placed close to the PD to minimize current consumption and to get sufficient signal for detecting heart rate.

The sensor can be placed freely on any body part that has microvascular tissue, but for convenient and practical use, the sensor was placed on the upper arm to measure optical heart rate and SpO_2 of the participant. This location might also have less interference when performing physical activities while also providing proven accuracy. In previous research, the upper arm has been shown to be a good and comfortable location for optical heart rate measurements [5].

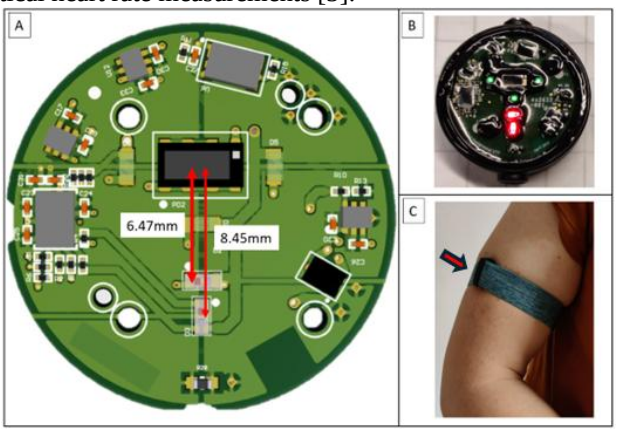

Fig. 1. A: Layout of the circuit board with distances from IR/RED to PD. B: Picture of the device with injection molded lens. A screen page corresponds to 7 mm. More information in the next chapter. C: Device (arrow pointing the sensor) on author's upper arm. The sensor is strapped comfortably to the arm.

The PPG device is an embedded system which incorporates all the optical components, driver, and control electronics integrated into a hard case packaging for multiple wavelength PPG measurement. The optical head comprises a photodetector (VEMD 8080) and surface mount LEDs at green (525 nm), red (655 nm) and IR (940 nm) wavelengths. Three green LEDs are placed around the PD with a center-to-edge distance of 2 mm. Two integrated dual-wavelength red and IR LED (Osram SFH 7015) are used for SpO2 measurement, one of which is placed in parallel and the other perpendicular to the photodetector (PD). The different orientation was arranged to investigate the impact of the LED-to-PD orientation on the optical response. The distal and proximal dual-wavelength LEDs are placed at center-to-center distances of 8.45 mm and 6.27 mm from the PD, respectively. See Fig. 1, where the circuit board, a picture of the device and a volunteer wearing the sensor can be seen.

The photodiode was reversely- biased at 1.485 V to operate in photoconductive mode. This decreases the capacitance of the PD, widens the depletion region and improves the absorption of the incident photons. The LEDs and PD are driven by a dedicated mixed-signal frontend (ADPD4100) to control the pulse specification and collect the optical current from the PD. Sampling rate was set to 23 Hz and bit width was 22bit. The whole system is driven by a high-performance, Bluetooth-enabled ARM processor (nRF5280 SoC). An integrated memory chip facilitates data storage for long-term data recording. The PPG system provides both USB and wireless (BLE) interfaces to read back the recorded data and configure the device.

The PPG electronics was realized on a 6-layer, high-density interconnect (HDI) PCB with an overall thickness of 0.8 mm. The system is supplied by a 45-mA rechargeable lithium polymer (LiPo) battery.

B. *Dispensing of the optical barrier and lenses*

The optical head of the PPG device was covered with adhesives to minimize crosstalk between LED emission and PD for optimal performance. In addition, a 3D-printed O-ring part with an adhesive sealing was utilized between the assembled PCB and the housing to create a waterproof enclosing. First, UV-curable black adhesive (Vitralit 1605 MV black from Panacol), which acted as a light barrier, was dispensed around the optoelectronic components. After curing, the UV-curable transparent adhesive (Vitralit 1605 from Panacol), which acted as an optical lens layer, was dispensed on the assembled PCB to fill all cavities of PD, LEDs, and the board. The black adhesive was deposited on the optical head with the dispensing method (Dima Elite Dispenser DR-61 dispensing robot (See Fig. 2)), whereas the transparent adhesive was dispensed manually. Both adhesive types meet the ISO 10993-5 requirements.

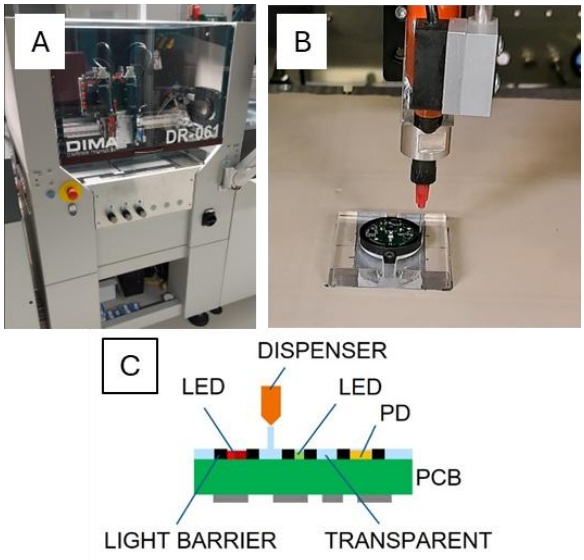

Fig. 2. A: Dispensing robot, B: The dispensing head, and C: A schematic picture showing light barrier and dispensing transparent lens.

C. *Sensor verification*

First, a user interface was developed to allow for data handling, data download, firmware updating, and changing settings in the analog front end controlling the optical measurement. Data communication was from the USB, but also a wireless graphical interface was developed for Android to see the data in real-time from a mobile phone. Several iterations were made to get the system fully operational.

Ten prototypes were manufactured, and each prototype was inspected visually and with a microscope to confirm that manufacturing was successful. Next, the light barriers were tested to ensure that they worked properly. A crosstalk test was done by placing the device optics facing up towards several meters of empty space (i.e. no optical reflections from objects) and the results showed that there was no DC signal measured by the sensor when the device was operating with all LEDs on. Reference for this measurement was a prototype without lens. When all the LEDs and the PD are in the same optical plane the crosstalk is nonexistent. Then, the AFE settings were optimized such that the signal quality of the sensors remained high, and the battery consumption was sufficient for measuring SpO_2 for several hours (for more than the duration of the study protocol).

Integrating sphere Ophir IS1.5-VIS-FPD-800 together with Ophir NOVA II power meter, was used to measure relative output power of the LEDs. Without the lens with bare circuit board, the light power was 1.96 mW. With the dispensed lens, the light power was 1.20 mW. The dispensed lens resulted in acceptable light power loss, especially as the light leakage is below the baseline level of noise.

The ambient rejection was checked by using external ambient halogen light source calibrated close to sunlight intensity around 30k klx (value is based on field testing measurements of sunlight in Finland at summertime). This test was successful, and no significant ambient noise was present. The sensor had one green channel (used to measure heartrate) and two channels were reserved for SpO_2 (long distance and short distance). An adaptation algorithm “autogain” which adjusts AFE’s gain settings was developed to allow the device to adapt to skin pigmentation variation. Results were confirmed by checking the sensor’s functionality on individuals with light and dark skin tones (Fitzpatrick scale levels 2 and 4 [28]), and the device achieved high AC and SNR levels. Signal analysis was done with an in-house developed MATLAB program (MATLAB 9.10.0.2198249 (R2021a) Update 8, The MathWorks, Inc., Natick, Massachusetts, United States). Moreover, some field tests with SpO_2 were conducted to investigate functional performance of the sensor. After all tests, sensors were ready for external data collection and provided with a user manual.

D. *Data collection for HR and SpO_2 Validation*

1) *Ethical Approval*

This research received prior approval from the University of Calgary Conjoint Health Research Ethics Board (Protocol #REB22-0153) and aligned with the Mount Royal University Human Research Ethics Board (Protocol #103225). The recruitment process and protocol adhered to the guidelines outlined in the Canadian Government Tri-Council Policy Statement and the Declaration of Helsinki. Although this study adhered to ethical standards, it was not formally registered as a clinical trial.

2) *Participants*

Twenty-eight healthy individuals between 18 and 40 years who were nonsmokers, had a BMI<30 $kg \cdot m^{-2}$, no underlying cardiac, respiratory, metabolic, or neurological disorders/diseases, and were not taking any medications related to these conditions were recruited for this study. Participants completed a medical screening questionnaire to confirm study eligibility, which a physician reviewed before participation.

The Fitzpatrick Skin Type Scale [28] was used by the participants to self-assess their skin type, with Type I being considered ivory white, and Type VI being considered very dark brown (Fig. 3). Fig. 3 (a) shows the frequencies for n=28 and Fig. 3 (b) shows the frequencies for n=25.

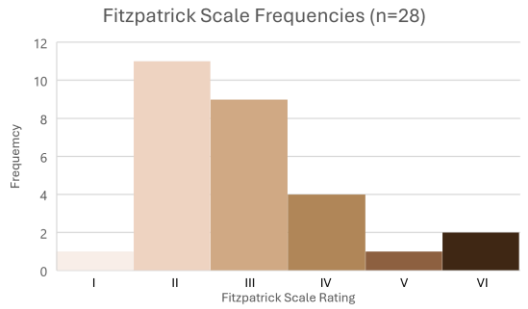

(a)

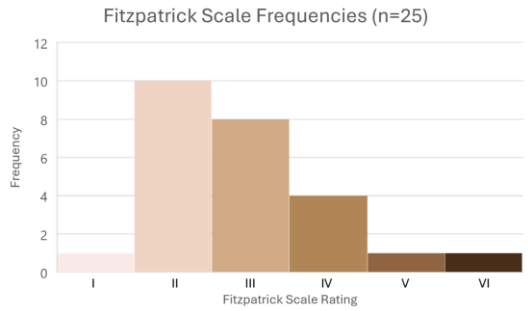

(b)

Fig. 3. Fitzpatrick Scale. (a) n=28, (b) n=25.

Out of the 28 participants, three had to be excluded from final analysis. The exclusions were due to technical failure in one case, the multiwavelength PPG sensor failed to register data and in the remaining two cases, the reference ECG recording encountered a technical issue and recorded erroneous data for the length of the protocol.

Participant demographics and laboratory conditions are reported in Table 1.

TABLE 1. PARTICIPANT DEMOGRAPHICS AND TESTING CONDITIONS INFORMATION.

	All (n=25)	Male (n=16)	Female (n=9)
Demographic Information			
Age (yr)	27.6 ± 4.1	27.5 ± 4.6	27.7 ± 3.4
Height (cm)	161.8 ± 9.5	178.1 ± 8.5	165.8 ± 5.35
Weight (kg)	71.8 ± 11.6	78.1 ± 8.2	60.6 ± 7.5
BMI ($kg \cdot m^{-2}$)	23.7 ± 2.5	24.7 ± 2.5	22.1 ± 1.7
Skin type (1-6)	3 (1-6)	3 (1-6)	2 (2-3)
Testing Conditions			
Ambient Temperature (°C)	20.8 ± 0.8	20.7 ± 0.8	21.1 ± 0.8
Ambient Humidity (%)	17.4 ± 3.6	16.8 ± 3.9	18.3 ± 2.7
Ambient Pressure (mmHg)	659.5 ± 5.1	659.5 ± 4.6	659.5 ± 6.0

3) *Experimental protocol*

This study followed the ISO protocol (ISO 80601-2-61;2017) for evaluating and documenting the SpO_2 accuracy of pulse oximeter equipment [29]. Data were collected during a single testing session at the Canadian Sport Institute Alberta (altitude: 1130m; atmospheric pressure (P_{ATM}): ~660 mmHg). Upon participant arrival at the laboratory, testing procedures were explained along with possible risks before participants provided free, informed verbal and written consent. Resting HR and blood pressure were measured.

Participants were instrumented with the multiwavelength PPG sensor while resting in a supine position. The device was attached to the lateral aspect of the participant's upper arm using an adjustable strap, approximately halfway between the shoulder and the elbow. To allow the multiwavelength PPG sensor to accommodate skin temperature, the device was secured on the participant's arm by a researcher at least 15 minutes prior to data collection. Participants were offered an anti-static blanket to help reduce PPG SpO_2 measurement errors due to reduced peripheral blood flow from cold body temperature.

To follow regulated safety procedures, participants wore a fingertip pulse oximeter (ADI oximeter pod, ML 320 and Nonin® 8000AA finger probe, ADI MLT 321) on their middle finger. Blood draws were taken with a radial arterial catheter in the contralateral wrist from the devices to analyze SaO_2. Based on accessibility of the radial artery and participant comfort, an anesthesiologist or respiratory therapist determined which wrist to insert the catheter. A mouthpiece was used to deliver specific gas concentrations from 200 L Douglas bags (0.18, 0.16, 0.14, 0.12 F_IO_2). Cardiorespiratory data were collected using an analog to digital data acquisition system (PowerLab/16SP ML880; ADI; sampling frequency: 1000 Hz). A gas sample line was connected to the mouthpiece to measure and calculate the fraction of inspired (F_I), fraction of expired (F_E) and pressure of end-tidal oxygen ($P_{ET}O_2$) and pressure of end-tidal carbon dioxide ($P_{ET}CO_2$) using a dual gas analyzer (ADI ML 206) Electrocardiography (ECG) electrodes (ECG: lead II configuration; ADI Bioamp ML 132) measured continuous HR over the testing session. Nonin® fingertip SpO_2 data, cardiorespiratory measures, and ECG signals were monitored during the testing session, and archived and analyzed offline using ADI LabChart Pro software (v8.0). During blood sample periods, participants were instructed to minimize movement to limit motion artifacts in the SpO_2 measurements.

4) *Data Collection*

Once the participant was fully instrumented and comfortable, the data collection systems were synchronized by starting the multiwavelength PPG sensor and LabChart Pro software (v8.0) after a 3-second countdown. The mouthpiece was in the mouth of the participant. The participant then breathed ambient air (0.21 F_IO_2) for ~5 minutes before the first set of five blood samples were drawn. All blood samples were processed within ten minutes using a portable blood gas/electrolyte machine (i-STAT; Abbott, Mississauga, Ontario, Canada) for analysis of $PaCO_2$, PaO_2, and SaO_2. Following the first set of blood samples, the inspired gas was then switched to the next hypoxic gas stage, and participants were allocated a ~4-minute interval to achieve steady state, characterized by a qualitatively stable and unchanging pressure of end-tidal carbon dioxide ($P_{ET}CO_2$),

oxygen ($PETO_2$) and SpO_2 (ADI/Nonin®) which was continuously evaluated by the experimenters. Following this stabilization period, a sequence of five consecutive arterial blood draws was conducted over approximately 2 minutes. This process was repeated for 0.18, 0.16, 0.14, and 0.12 F_IO_2 in a descending stepwise manner, with each step lasting approximately 6 minutes. After the 0.12 F_IO_2 stage, a 3-minute washout period of breathing ambient air was completed before participants removed the mouthpiece.

E. Data-analysis for HR accuracy

The initial stage of the data-analysis process involved the calculation of raw HR readings derived from the PPG channels from the multiwavelength PPG sensor. This computation employed a proprietary signal processing algorithm.

Subsequently, the HR data was resampled to a frequency of 1 Hz by using linear interpolation to align with the reference signal. The signals were then manually synchronized by identifying and adjusting the offset. To enhance accuracy, synchronization between signals was double-checked by computing the difference of signals in 10-second windows. This approach effectively eliminated potential variations in delays caused by hardware or software.

The accuracy between the multiwavelength PPG sensor and reference signal values was assessed by calculating root mean squared error (RMSE). The data processing was performed with custom-made MATLAB software (MATLAB 9.10.0.2198249 (R2021a) Update 8, The MathWorks, Inc., Natick, Massachusetts, United States).

F. Data analysis for SpO_2

1) Data Processing

Blood draw event markers were created in ADI/LabChart Pro software (v8.0) at the exact time points when each arterial blood draw was obtained. The ISO 80601 protocol outlines validation for SaO_2 values between 70 and 100%, so any blood samples with SaO_2 values below 70% were removed from the final analysis. Data processing was performed in two parts. Part A included SpO_2 and SaO_2 data of 25 participants. Part B included a randomly chosen subset of 13 participants.

2) Part A: Multiwavelength PPG sensor SpO_2 Validation

For the comparison of SpO_2 with SaO_2 data, all SpO_2 data from the multiwavelength PPG sensor were imported into a custom MATLAB code. The multiwavelength PPG sensor signal quality of the perfusion ratio was estimated with proprietary statistical metrics (herein referred to as "quality estimate") that were based on the estimation of experimentally defined physiological limits. If the data point was outside the quality limits, then it was assumed not to be of physiological origin and therefore deemed as poor quality and excluded. Blood draw event markers from the ADI/LabChart Pro software (v8.0) were identified in the multiwavelength PPG sensor SpO_2 dataset. Subsequently, data were averaged over a 7-second interval around each arterial blood draw event marker, considering potential delays in manually starting and stopping the device testing at the initiation and conclusion of data collection periods.

This process resulted in five paired SaO_2 and SpO_2 values for each oxygen step for the multiwavelength PPG sensor. The comparisons between SaO_2 and SpO_2 were conducted using data measured from the multiwavelength PPG sensor to evaluate its accuracy in relation to blood draws.

3) Part B: Multiwavelength PPG sensor SpO_2 Algorithm Re-Calibration

SaO_2 data from a randomly chosen subset of 13 participants were forwarded to blinded researchers with the aim of refining the SpO_2 algorithm to enhance accuracy levels. A researcher imported this dataset into MATLAB and applied the proprietary multiwavelength PPG sensor SpO_2 calibration algorithm. The evaluators of the test data set were completely blind to these participants during the re-training. To ensure temporal alignment, the initial algorithm results and corresponding SaO_2 data were synchronized by cross-referencing timestamps recorded by both devices (multiwavelength PPG sensor and ADI/LabChart Pro software, v8.0).

A new set of calibration values was generated from the relationship between the initial uncalibrated data and SaO_2 data established by the calibration algorithm. These calibration parameters were then incorporated into the proprietary multiwavelength PPG sensor SpO_2 calculation algorithm. Subsequently, SpO_2 values were recalculated for the remaining 12 participants whose SaO_2 data had not been shared with blinded researchers. The updated multiwavelength PPG sensor SpO_2 results were returned to the non-blinded research team for an objective comparison with SaO_2 data.

4) Statistical Analyses

The statistical analysis of HR accuracy and SpO_2 accuracy was based on the same parameters. The ISO 80601 protocol outlines the use of RMSE to assess the accuracy of pulse oximeter equipment. Thus, the accuracy of the multiwavelength PPG sensor data compared to the SaO_2 measurements was first assessed using the following equation (1):

$$RMSE = \sqrt{\frac{\sum_{i=1}^{n}(SpO_2 - SaO_2)^2}{n}} \quad (1)$$

To assess agreement between paired measurements, intraclass correlation coefficients (ICCs) were calculated for each participant in SPSS Version 28 (IBM, Houston, Texas, USA) using a single measurement, absolute agreement, two-way mixed effects model. ICCs were categorized as poor (<0.4), moderate (0.4–0.75), or excellent (>0.75) based on established criteria [30]. Additionally, Pearson correlation coefficients (r) were computed to gauge the strength of the relationship between SpO_2 and SaO_2 values. Finally, error distribution concerning the mean difference between SpO_2 and SaO_2 values was assessed using Bland-Altman plots (mean difference, limits of agreement (LOA)).

Given the repeated measures nature of the study, correlations, Bland-Altman analyses, and ICCs using an average measurement, absolute agreement, two-way mixed effects model was also conducted on averaged data points from

each participant (i.e., five SaO_2 - SpO_2 data pairs averaged over each O_2 step, resulting in five data points per participant over the entire data collection). The results were highly consistent; thus, reported correlations, Bland-Altman analyses, and ICCs encompassed all data points.

For reflectance pulse oximetry equipment to be considered valid according to ISO 80601 protocol, SpO_2 accuracy should yield an RMSE value of ≤4% across the entire SaO_2 range of 70-100%. The ISO protocol also recommends providing accuracy specifications for SaO_2 ranges: 70-79.9%, 80-89.9%, and 90-100%. Hence, analyses were initially conducted over the full SaO_2 range (70-100%) for the multiwavelength PPG sensor (Parts A & B). SpO_2 measures were considered accurate for a specific SaO_2 range if the RMSE was ≤4%.

III. Results

A. HR accuracy study

The average RMSE over all the participants was 1.6 ± 1.1 % (Table 2). The largest RMSE was observed with participant S28 that had an RMSE of 4.59 % (Table 2). The ECG-derived heart rate and the PPG-derived heart rate of the case S13 is presented in Fig. 4 and of the case S19 is presented in Fig. 5. In the most accurate case, the RMSE was 0.66 % (Table 2). Fig. 6 depicts Bland-Altman analysis of HR between multiwavelength PPG sensor and ECG-derived reference.

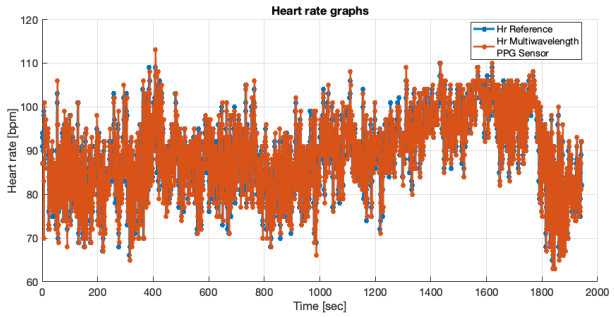

Fig. 4. Accuracy below average, case S13.

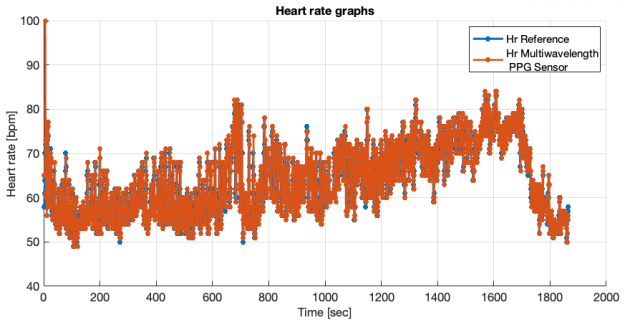

Fig. 5. Accuracy above average, case S19.

B. SpO_2 Validation Study

Values are reported for 25 participants included in data analyses and are expressed as mean ± SD. Root mean square error (RMSE) for measured SpO_2 values compared to SaO_2 reference values. Figure 7 depicts an example of multiwavelength PPG sensor measurement result with the sensor prototype and the blood draws as a reference. Data for a wrist unit from the study has been published elsewhere [17].

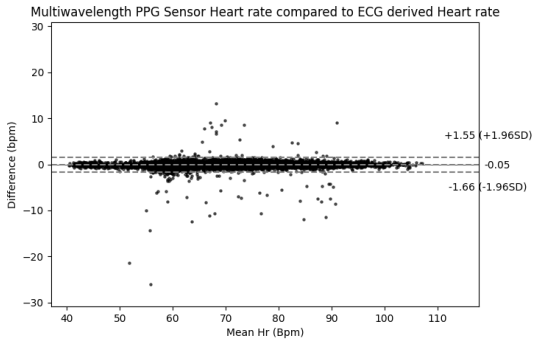

Fig. 6. Bland-Altman analysis of HR between multiwavelength PPG sensor and ECG derived reference.

TABLE 2. ACCURACY OF MULTIWAVELENGTH PPG SENSOR HR AT REST

Participant ID	Average HR (bpm)				Correlation
	Multi-wavelength PPG sensor	*ICC*	*Multi-wavelength PPG sensor*	*Reference*	*r (p<0.05)*
S1	1.12	0.95	74.98	74.99	0.96
S2	1.01	0.99	86.52	86.53	0.99
S3	1.98	0.96	61.98	61.82	0.96
S4	3.17	0.95	63.77	63.52	0.95
S5	1.59	0.98	65.59	65.59	0.98
S6	0.83	0.98	75.92	75.91	0.99
S7	0.95	0.99	79.27	79.26	0.99
S8	0.94	0.99	86.13	86.12	0.99
S9	1.02	0.73	64.41	64.32	0.77
S10	0.66	0.99	78.49	78.47	0.99
S12	1.19	0.98	57.61	57.52	0.98
S13	2.64	0.96	89.70	89.74	0.96
S14	1.20	0.97	46.45	46.36	0.98
S15	1.31	0.99	67.14	67.10	0.99
S16	1.32	0.98	74.67	74.72	0.99
S18	1.09	0.98	78.72	78.71	0.99
S19	0.78	0.99	64.38	64.41	0.99
S20	1.28	0.80	69.19	69.18	0.93
S21	2.10	0.97	87.98	87.89	0.97
S22	1.00	0.99	80.83	80.83	0.99
S23	1.91	0.98	74.25	74.22	0.98
S24	4.58	0.76	66.15	66.03	0.75
S26	1.44	0.97	76.24	76.37	0.97
S27	1.27	0.99	69.18	69.11	0.99
S28	4.59	0.81	86.04	85.77	0.81
Average ± SD	**1.64± 1.06**	**0.95± 0.08**	**73.02± 10.6**	**72.98± 10.6**	**0.95± 0.07**

The multiwavelength PPG sensor (Part B) RMSE values were calculated for the participants whose SaO_2 data was not sent to blinded researchers for algorithm recalibration (n=13).

Table 3 depicts the accuracy of multiwavelength PPG sensor SpO_2 at rest (Part A) and Fig. 8 shows corresponding graphs. Table 4 depicts accuracy of multiwavelength PPG sensor SpO_2 at rest (Part B) and Fig. 9 shows corresponding graphs. Fig. 10 compares results of Part A and Part B.

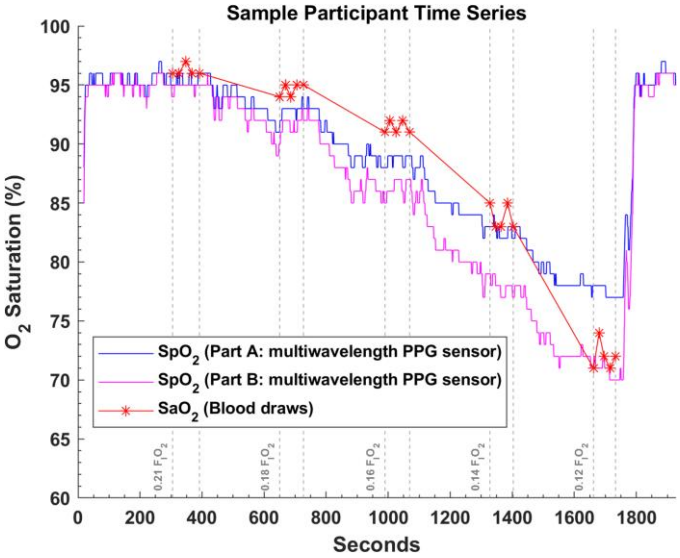

Fig. 7. Sample participant time series plot displaying continuous SpO_2 estimation by multiwavelength PPG sensor device (Part A, blue; Part B, purple), and discrete SaO_2 values (red).

IV. Discussion

Because pulse oximetry is a well-accepted technology in daily clinical practice, there are strict guidelines for the device manufacturers to validate the accuracy of the devices before entering the market. Guidance for the validation is provided in the ISO standard [29]. The accuracy of the device is also important in wellness and sport use. Therefore, we analyzed the accuracy of this wearable sensor against the gold standard – arterial blood sample reference. Reflectance style SpO_2 measurement from wrist and a fingertip pulse oximeter (ADI/Nonin®) were recently compared by Russell et al. [17]. Differences in the accuracy can be understood by the operation principle, where the fingertip sensor measures transmitted optical signal, while the multiwavelength PPG sensor uses a reflectance measurement configuration. It is known that the accuracy requirements are different for those styles (i.e., transmittance vs. reflectance) [27]. Also, the upper arm position is not as prone to motion artifacts as the wrist in the reflectance style measurement [21]. An important aspect for considering benefits and drawbacks of different approaches is the wearability of the multiwavelength PPG sensor. Wearing the sensor on the arm enables daily activity and HR monitoring without limiting the use of the hands, unlike a similar fingertip sensor that would likely create discomfort over long periods of time.

This paper advances several topics mentioned in the recent roadmap paper for PPG research [31]. Biosafety was considered by using adhesive materials meeting the ISO 10993-5 requirements. The new type of manufacturing of optical lenses also shows that minimizing the optical pathlength from LED to skin increases the optical power entering the skin and then gives possibilities for LED current and battery consumption optimization. The optical configuration uses LEDs at different distances and orientation. With help of multiple wavelengths, this gives more flexibility for algorithm development and taking care of motion artifacts.

Table 3. Accuracy of multiwavelength PPG sensor SpO_2 at rest (part A).

Participant ID	*RMSE*	*ICC*	**Correlation *r (p=0)***
S1	5.44	0.725	0.977
S2	0.93	0.984	0.984
S3	1.02	0.942	0.956
S4	3.34	0.888	0.964
S5	3.17	0.919	0.955
S6	1.82	0.955	0.98
S7	2.96	0.903	0.975
S8	4.05	0.773	0.98
S9	1.39	0.946	0.964
S10	3.10	0.924	0.968
S12	2.96	0.912	0.949
S13	3.66	0.886	0.984
S14	4.11	0.822	0.98
S15	4.24	0.842	0.963
S16	2.09	0.931	0.974
S18	2.03	0.937	0.965
S19	2.45	0.938	0.943
S20	1.83	0.793	0.935
S21	3.82	0.829	0.975
S22	3.78	0.887	0.975
S23	2.75	0.932	0.981
S24	4.37	0.828	0.981
S26	3.78	0.873	0.939
S27	2.45	0.916	0.98
S28	6.55	0.633	0.978
Average ± std	**3.12±1.33**	**0.877±0.081**	**0.968±0.015**

Commercial straps were used to attach the sensor, which were previously shown to improve customer satisfaction. The placing of the sensor was adjusted to the arm to provide a good PPG signal quality. In addition to the demonstrated SpO_2 and HR measurement accuracy, our sensor provides several important aspects of consumer applications, like wearability and connection to a mobile application to allow for easy access to sensor measurements by the user.

This sensor achieves an RMSE of 3.12% with a 7-second moving average analysis for 25 participants. When re-training the algorithm, the achieved RMSE was 2.61%, which is well within the limits of ISO standard (<4%) and FDA requirements

(<3.5%). Recalibration of the sensor (Fig. 10) reduced the overestimation of SpO_2 values at low range and improved accuracy. This is very important in different applications of elite and endurance athletes, where SpO_2 varies in a large range [32],[33],[34],[35].

TABLE 4. ACCURACY OF MULTIWAVELENGTH PPG SENSOR SpO_2 AT REST (PART B).

Participant ID	*RMSE*	ICC	Correlation *R (p=0)*
S2	2.70	0.905	0.982
S3	1.73	0.877	0.954
S4	2.47	0.951	0.963
S5	2.82	0.949	0.957
S8	5.59	0.708	0.985
S9	1.46	0.954	0.961
S10	4.02	0.908	0.971
S13	1.57	0.982	0.986
S14	2.01	0.963	0.983
S24	3.13	0.927	0.979
S27	1.24	0.982	0.983
Average ± std	**2.61±1.29**	**0.919±0.077**	**0.973±0.012**

The optical response to declining blood oxygen level varies between individuals and this variation cannot be explained by skin tone in this study. The optical response measured by our multiwavelength PPG device appears to have different baselines (signal levels at ambient air) between individuals and slightly different rates of change. To improve the overall accuracy and to decrease the inter-individual variation the algorithm would benefit from the larger group of participants and wider demographics. To improve the sensor, more thorough mechanical and electrical testing at different temperatures and levels of humidity should be conducted.

An SpO_2 feature has been implemented on several consumer grade devices, but the devices show varying results on validity in high altitude applications and needs special attention [36],[37],[38]. Wearable wrist worn devices have shown clinical accuracy in hypoxia study as well as in identifying apnea and hypopnea events [14]. The consumer devices have also shown applicability in patients with cardiovascular or lung diseases and in healthy subjects [39]. Here we show that a wearable arm band sensor can measure heart rate optically with high accuracy. At the same time, it provides an excellent potential SpO_2 sensor for monitoring purposes in sport domains.

One limitation of the selected measurement site includes the lower perfusion of the skin in comparison to peripheral sites like the finger, palm or ear [40]. Moreover, peripheral vasoconstriction is more prominent in cold environments such as diving in cold water that could affect the measurements from the sensor [41]. However, the compact and versatile design of the device allows it to be used on different body locations. For example, the forehead could be a suitable location for SpO_2 measurement with this device to monitor falling oxygen levels during underwater diving [42].

Cold environment also introduces further challenges in terms of usability. Using the device outdoors may be difficult because the upper arm's skin surface is not easily accessible when wearing long sleeved outdoor clothing. This limitation could be addressed by incorporating remote control functionality.

We expect that the wellness SpO_2 monitoring applications of wearable devices will increase when validated devices will be available in consumer market [43],[44].

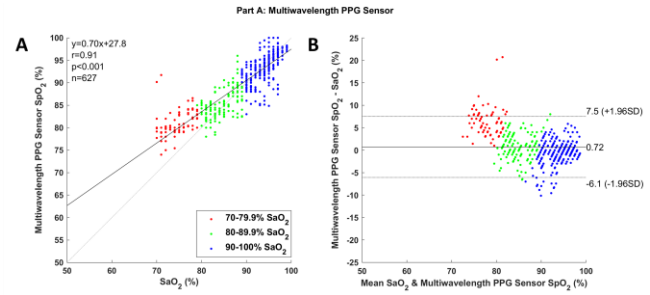

Fig. 8. Part A results of multiwavelength PPG sensor prototype.

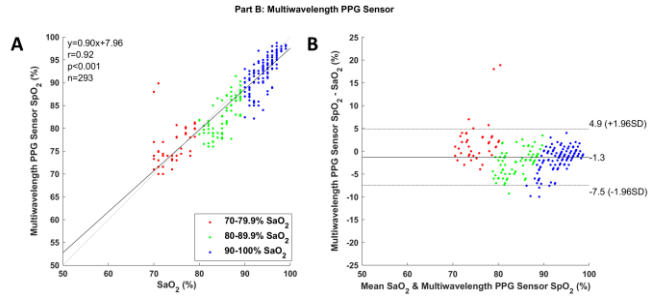

Fig. 9. Part B results of multiwavelength PPG sensor prototype.

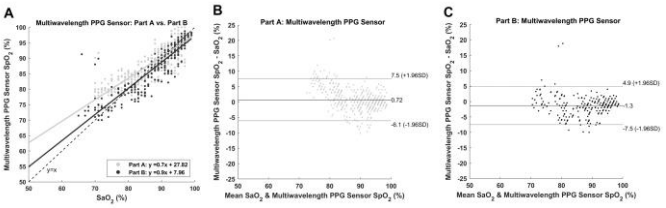

Fig. 10. Comparison of Part A and Part B results.

V. CONCLUSION

This study characterizes the development and validation of a wearable sensor for measuring OHR and SpO_2. The advanced technology of dispensing the lenses and cover of the optical sensor head provided good results and the accuracy of the sensor meets the requirements of standards required for medical use. With a novel dispensed lens, three targets were achieved; 1) close distance between skin and LED and PD; 2) high AC and SNR; and 3) optical layout with two SpO_2 channels (short and long distance) and one OHR channel. OHR and SpO_2 analysis showed excellent performance of the sensor during the experiment. When a sensor is placed on the upper arm, it does not interfere with daily tasks, so a wide range of applications are foreseen for this sensor in the wellness and health domain, where accurate data are needed.

REFERENCES

[1] R. J. Shei, I. G. Holder, A. S. Oumsang, et al. "Wearable activity trackers–advanced technology or advanced marketing?," *Eur. J. Appl. Physiol.*, vol. 122, pp. 1975–1990, 2022.

[2] R. Al-Halawani, P. H. Charlton, M. Qassem, and P. A. Kyriacou, "A review of the effect of skin pigmentation on pulse oximeter accuracy," *Physiol. Meas.*, vol. 44, 05TR01, 2023.

[3] B. Bent, B. A. Goldstein, W. A. Kibbe, et al. "Investigating sources of inaccuracy in wearable optical heart rate sensors," *npj Digit. Med.*, vol. 3, no. 18, 2020.

[4] M. E. Haveman, M. C. van Rossum, R. M. E. Vaseur, C. van der Riet, R. C. L. Schuurmann, H. J. Hermens, J. P. M. de Vries, M. Tabak, "Continuous Monitoring of Vital Signs With Wearable Sensors During Daily Life Activities: Validation Study, " *JMIR Form Res.*, vol. 6, no. 1, e30863, Jan. 2022.

[5] I. T. Hettiarachchi, S. Hanoun, D. Nahavandi, S. Nahavandi, "Validation of Polar OH1 optical heart rate sensor for moderate and high intensity physical activities, " *PLoS One*, vol. 14, no. 5, e0217288, May 2019.

[6] I. Mujika, A. P. Sharma, T. Stellingwerff, "Contemporary Periodization of Altitude Training for Elite Endurance Athletes: A Narrative Review," *Sports Med.*, vol. 49, no. 11, pp. 1651-1669, Nov. 2019.

[7] F. de. Asís Fernández. L. Rodríguez-Zamora, and E. Schagatay, "Hook Breathing Facilitates SaO2 Recovery After Deep Dives in Free divers With Slow Recovery," *Frontiers in physiology*, vol. 10, 1076, Aug. 2019.

[8] Z. Zhang, M. Qi, G. Hügli, R. Khatami, "The Challenges and Pitfalls of Detecting Sleep Hypopnea Using a Wearable Optical Sensor: Comparative Study," *J. Med Internet Res.*, vol. 23, no. 7, e24171, Jul 2021.

[9] A. Jubran, "Pulse oximetry," *Critical Care*, vol. 19, no. 272, 2015.

[10] M. Nitzan, A. Romem, R. Koppel, "Pulse oximetry: fundamentals and technology update," *Med Devices (Auckl)*, vol. 8, no. 7, pp. 231-239, Jul. 2014.

[11] M. Nuhr, K. Hoerauf, A. Joldzo, N. Frickey, R. Barker, L. Gorove, T. Puskas, and A. Kober, "Forehead SpO_2 monitoring compared to finger SpO_2 recording in emergency transport," *Anaesthesia*, vol. 59, pp. 390-393, 2004.

[12] E. Shebl, P. Modi, T. D. Cates, (Jan. 2023) "Home Oxygen Therapy," [Updated 2023 May 29]. In: StatPearls [Internet]. Treasure Island (FL): StatPearls Publishing; Available : https://www.ncbi.nlm.nih.gov/books/NBK532994/

[13] F. Rincon, J. Pidoux, S. Murali, et al. "Performance of the new SmartCardia wireless, wearable oximeter: a comparison with arterial SaO_2 in healthy volunteers," *BMC Anesthesiol*., vol. 22, 77, 2022.

[14] R. Kirszenblat, and P. Edouard, "Validation of the Withings ScanWatch as a Wrist-Worn Reflective Pulse Oximeter: Prospective Interventional Clinical Study," *J. Med. Internet Res.*, vol. 23, no. 4, e27503, 2021.

[15] J. Rafl, T. E. Bachman, V. Rafl-Huttova, S. Walzel, and M. Rozanek, "Commercial smartwatch with pulse oximeter detects short-time hypoxemia as well as standard medical-grade device: Validation study," *Digit Health.*, Oct. 2022.

[16] S. Marinari, P. Volpe, M. Simoni, M. Aventaggiato, F. De Benedetto, S. Nardini, C. M. Sanguinetti, P. Palange, "Accuracy of a New Pulse Oximetry in Detection of Arterial Oxygen Saturation and Heart Rate Measurements: The SOMBRERO Study," *Sensors*, vol. 22, no. 13, 5031, Jul. 2022.

[17] M. K. Russell, J. F. Horton, C. A. Clermont, J. M. Demarty, L. C. Transfiguracion, B. R. Worobets, M. E. Pineda, N. Santaniemi, P. Stergiou, M. J. Asmussen, T. A. Day, "Validation of Polar ElixirTM Pulse Oximeter against Arterial Blood Gases during Stepwise Steady State Inspired Hypoxia," Medicine & Science in Sports & Exercise, April 2024.

[18] M. M. Schubert, A. Clark, and A. B. De La Rosa, "The Polar ® OH1 Optical Heart Rate Sensor is Valid during Moderate-Vigorous Exercise," *Sports Med. Int. Open*, vol. 2, no. 3, E67-E70, Jun. 2018.

[19] J. W. Navalta, D. W. Davis, E. M. Malek, B. Carrier, N.G. Bodell, J. W. Manning, J. Cowley, M. Funk, M. M. Lawrence, and. M. DeBeliso, "Heart rate processing algorithms and exercise duration on reliability and validity decisions in biceps-worn Polar Verity Sense and OH1 wearables," *Sci. Rep.*, vol. 13, no. 1, 11736, Jul. 2023.

[20] E. Hermand, J. Cassirame, G. Ennequin, and O. Hue, "Validation of a Photoplethysmographic Heart Rate Monitor: Polar OH1," *Int. J. Sports Med.*, vol. 40, no. 7, pp. 462-467, Jul. 2019.

[21] Y. Maeda, M. Sekine, and T. Tamura, " Relationship Between Measurement Site and Motion Artifacts in Wearable Reflected Photoplethysmography," *J. Med. Syst*., vol. 35, pp. 969-976, 2011.

[22] J. Allen, "Photoplethysmography and its application in clinical physiological measurement," *Physiol. Meas.*, vol. 28, no. 3, R1, 2007.

[23] H. Lee, H. Ko, J. Lee, "Reflectance pulse oximetry: Practical issues and limitations," *ICT Express*, vol. 2, no. 4, pp. 195-198, Dec. 2016.

[24] M. Chan, V. G. Ganti, J. A. Heller, C. A. Abdallah, M. Etemadi, and O. T. Inan, "Enabling Continuous Wearable Reflectance Pulse Oximetry at the Sternum," *Biosensors*, vol. 11, 521, 2021.

[25] P. H. Charlton, P. A. Kyriacou, J. Mant, V. Marozas, P. Chowienczyk, and J. Alastruey, "Wearable Photoplethysmography for Cardiovascular Monitoring," *Proc. IEEE Inst. Electr. Electron. Eng.*, vol. 110, no. 3, pp. 355-381, 2022.

[26] F. Scardulla, G. Cosoli, S. Spinsante, A. Poli, G. Iadarola, R. Pernice, A. Busacca, S. Pasta, L. Scalise, and L. D'Acquisto, "Photoplethysmograhic sensors, potential and limitations: Is it time for regulation? A comprehensive review," *Measurement*, vol. 218, 113150, 2023.

[27] https://www.analog.com/en/technical-articles/guidelines-for-the-optomechanical-integration-of-heartrate-monitors-in-wearable-wrist-devices.html

[28] T. B. Fitzpatrick "Soleil et peau" [Sun and skin] [in French]. J. de Med. Esth. vol. 2, pp. 33-4, 1975.

[29] https://www.iso.org/standard/67963.html

[30] T. K. Koo, and M. Y. Li, "A Guideline of Selecting and Reporting Intraclass Correlation Coefficients for Reliability Research," *J. Chiropr. Med*.b vol. 15, no. 2, pp. 155-63, Jun, 2016.

[31] P. H. Charlton et al., "The 2023 wearable photoplethysmography roadmap," *Physiol. Meas.*, 44 111001, 2023.

[32] J. Rojas-Camayo, C. R. Mejia, D. Callacondo, et al. "Reference values for oxygen saturation from sea level to the highest human habitation in the Andes in acclimatised persons," *Thorax*, vol. 73, pp. 776-778, 2018.

[33] J. A. Sinex, and R. F. Chapman, "Hypoxic training methods for improving endurance exercise performance," *Journal of Sport and Health Science*, vol. 4, no. 4, pp. 325-332, 2015.

[34] I. Mujika, A. P. Sharma, and T. Stellingwerff, "Contemporary Periodization of Altitude Training for Elite Endurance Athletes: A Narrative Review," Sports Med., vol. 49, pp. 1651–1669, 2019.

[35] T. Dünnwald, R. Kienast, D. Niederseer, and M. Burtscher, "The Use of Pulse Oximetry in the Assessment of Acclimatization to High Altitude," *Sensors*, vol. 21, 1263, 2021.

[36] C. J. Lauterbach, P. A. Romano, L. A. Greisler, R. A. Brindle, K. R. Ford, and M. R. Kuennen, "Accuracy and Reliability of Commercial Wrist-Worn Pulse Oximeter During Normobaric Hypoxia Exposure Under Resting Conditions," *Res. Q. Exerc. Sport.*, vol. 92, no. 3, pp. 549-558, Sep. 2021.

[37] L. M. Schiefer, G. Treff, F. Treff, P. Schmidt, L. Schäfer, J. Niebauer, K. E. Swenson, E. R. Swenson, M. M. Berger, and M. Sareban, "Validity of Peripheral Oxygen Saturation Measurements with the Garmin Fēnix® 5X Plus Wearable Device at 4559 m," *Sensors*, vol. 21 no. 19, pp. 6363, Sep. 2021.

[38] E. Hermand, C. Coll, J.-P. Richalet, and F. J. Lhuissier, "Accuracy and reliability of pulse O_2 measured by a wrist-worn oximeter," *Int. J. Sports Med.*, vol. 42, no. 14, pp. 1268-1273, 2021.

[39] C. Spaccarotella, A. Polimeni, C. Mancuso, G. Pelaia, G. Esposito, and C. Indolfi, "Assessment of Non-Invasive Measurements of Oxygen Saturation and Heart Rate with an Apple Smartwatch: Comparison with a Standard Pulse Oximeter," *J. Clin. Med.*, vol. 11, pp. 1467, 2022.

[40] E. Tur, M. Tur, H. I. Maibach, and R. H. Guy, "Basal perfusion of the cutaneous microcirculation: measurements as a function of anatomic position," *J. Invest. Dermatol*., vol. 81, no. 5, pp. 442-446, 1983.

[41] Institute of Medicine (US) Committee on Military Nutrition Research; B. M. Marriott, and S. J. Carlson, Eds. (1996). *Nutritional Needs In Cold And In High-Altitude Environments: Applications for Military Personnel in Field Operations.* Washington (DC): National Academies Press (US); 1996. Available from: https://www.ncbi.nlm.nih.gov/books/NBK232865/ doi: 10.17226/5197

[42] R. M. Lance, M. J. Natoli, F. Di Pumpo, T. P. Beck, A. Gatrell, G. J. Brown, D. Schocken, and R. E. Moon, "The Dewey Monitor: Pulse Oximetry can Warn of Hypoxia in an Immersed Rebreather Diver in Multiple Scenarios," *Ann. Biomed. Eng.*, vol. *50, no.* 2, pp. 222–232, 2022.

[43] M. H. Vargas, et al. "Day-night fluctuation of pulse oximetry," *Rev. Invest. Clin.*, vol. 60, no. 4, pp. 303-310, 2008.

[44] R. E. Gries, and L. J. Brooks, "Normal Oxyhemoglobin Saturation During Sleep, How Low Does It Go?," *Chest*, vol. 110, no. 6 pp. 1489-1492, Dec. 1996.